Article

pubs.acs.org/Biomac

Redox-Responsive, Core-Cross-Linked Micelles Capable of On-Demand, Concurrent Drug Release and Structure Disassembly

Hua Wang, Li Tang, Chunlai Tu, Ziyuan Song, Qian Yin, Lichen Yin, Zhonghai Zhang, and Jianjun Cheng*

Department of Materials Science and Engineering, University of Illinois at Urbana-Champaign, 1304 West Green Street, Urbana, Illinois 61801, United States

Supporting Information

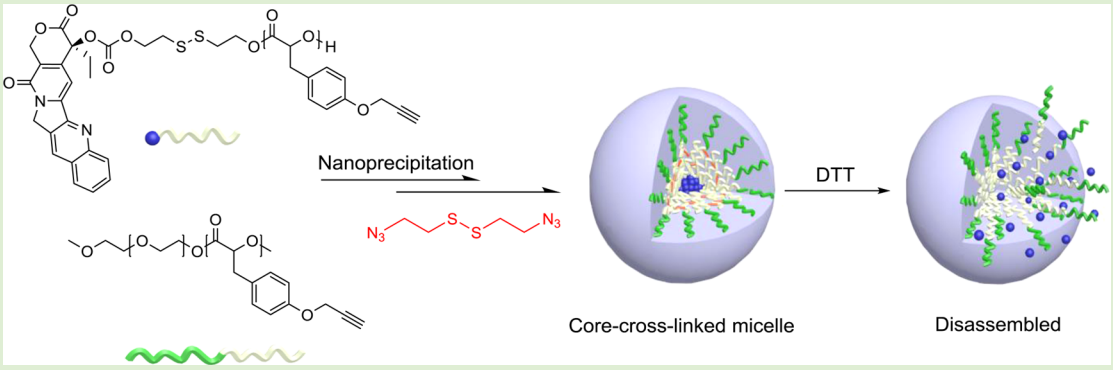

ABSTRACT: We developed camptothecin (CPT)-conjugated, core-cross-linked (CCL) micelles that are subject to redox-responsive cleavage of the built-in disulfide bonds, resulting in disruption of the micellar structure and rapid release of CPT. CCL micelles were prepared via coprecipitation of disulfide-containing CPT-poly(tyrosine(alkynyl)-OCA) conjugate and monomethoxy poly(ethylene glycol)-*b*-poly(tyrosine(alkynyl)-OCA), followed by cross-linking of the micellar core via azide–alkyne click chemistry. CCL micelles exhibited excellent stability under physiological conditions, while they underwent rapid dissociation in reduction circumstance, resulting in burst release of CPT. These redox-responsive CCL micelles showed enhanced cytotoxicity against human breast cancer cells in vitro.

INTRODUCTION

Polymeric micelles composed of a hydrophobic core and a hydrophilic shell are widely used as drug delivery vehicles for cancer therapy because they can increase the solubility and stability of the encapsulated or conjugated anticancer drugs, prolong drug circulation in the bloodstream, and improve the accumulation of drugs at disease site to minimize the side effects of the drugs.[1−6] The structure, composition, and core and surface property of micelles can be easily tuned through controlled polymerization and conjugation chemistry.[7,8] However, one issue central to the self-assembled micelles is their intrinsic instability under physiological conditions: micelles potentially undergo dynamic dissociation upon dilution and high shearing force in the circulation system in vivo.[9−12] Various approaches have been employed to improve the stability of micelles in the biological systems, including chemical cross-linking of the shell[13−16] or the core[17−20] of self-assembled micelles. Cross-linking of the micellar coronas leads to the formation of robust shell cross-linked micelles. However, one challenge of this approach is that cross-linking of the micellar shell generally requires highly diluted condition to avoid undesired intermicellar cross-linking, which potentially makes it difficult for large-scale production and materials handling.[21−23] Furthermore, cross-linking of the hydrophilic shell of micelles may result in decreased shell fluidity and hydrophilicity,[14,24,25] thus compromising the stealth effect and reducing the circulation time of micelles in the bloodstream. In comparison, core-cross-linking strategy can increase the stability of micelles with minimal impact on the micelle surface property and their blood circular half life.[26−28]

Apart from excellent extracellular stability, ideal drug carriers should also be capable of releasing the drugs in a temporally and spatially controlled manner in response to internal or external triggers.[29−31] Specific and rapid drug release at pathological sites could be potentially achieved using stimuli-responsive drug delivery system, minimizing the probability of drug resistance and systemic side effect.[32−34] Much effort has been devoted to the development of degradable micellar delivery systems that are responsive to intracellular changes of pH,[35−38] temperature,[39−41] glutathione (GSH),[38,42−44] and enzyme level.[45−49] The large concentration gradient of GSH between the intracellular (∼10 mM) and the extracellular

Received: July 24, 2013
Revised: August 30, 2013
Published: September 4, 2013

dx.doi.org/10.1021/bm401086d | *Biomacromolecules* 2013, 14, 3706−3712

Scheme 1. (a) Synthetic Route of CPT-*S*-*S*-poly(2) and mPEG-poly(2) and (b) Preparation of UCL and CCL Micelles

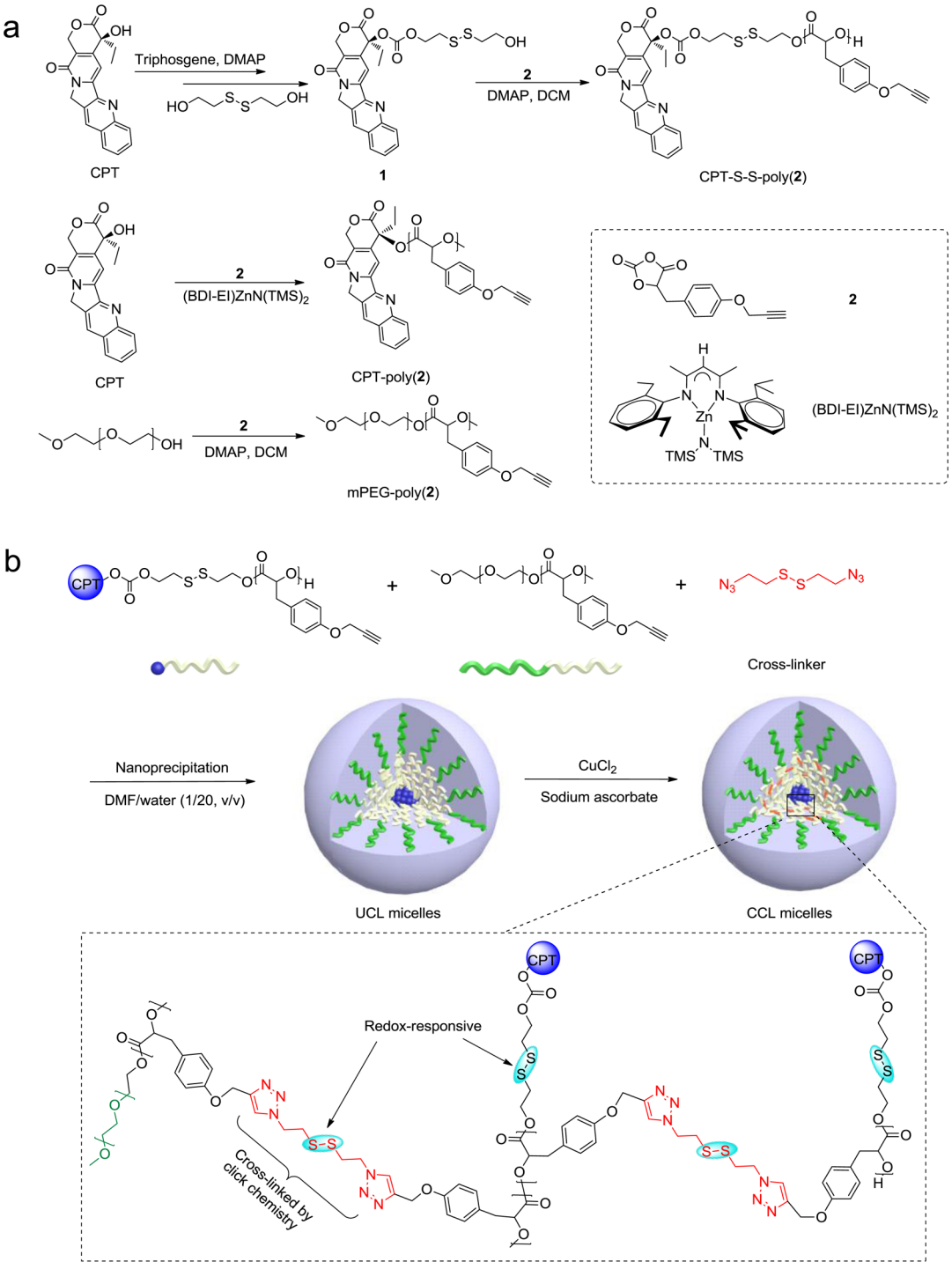

environment (~0.002 mM) is an ideal internal trigger for the design of redox-responsive micelles. These micelles remain stable during blood circulation with minimal drug release, while they disassemble rapidly and give burst drug release intracellularly. Cajot et al. reported disulfide-cross-linked micelles that displayed a slow drug release profile under physiological conditions but rapidly released the drug in a reductive environment, mimicking that of the cytoplasm and cell nucleus.[50] Jing[51] and other groups[52,53] have demonstrated the improved stability and therapeutic effects of redox-responsive core-cross-linked (CCL) micelles.

To address the outstanding challenge in micelle-based drug delivery of achieving highly stable micelles capable of on-demand drug release, we developed a CCL micelle that showed redox-responsive disruption of the micellar structure and concurrent cleavage of drug-polymer conjugate (Scheme 1). Because physically encapsulated drugs may inevitably encounter undesired leak and burst release problems upon blood dilution during circulation, we covalently conjugate camptothecin (CPT) to the core via a disulfide bond linker. CPT was first modified with a disulfide linker and then initiated ring-opening polymerization of 5-[4-(prop-2-yn-1-yloxy)benzyl]-1,3-dioxo-

dx.doi.org/10.1021/bm401086d | *Biomacromolecules* 2013, 14, 3706−3712

Table 1. Ring-Opening Polymerization of 2 (Tyr(alkynyl)-OCA)[a]

entry	initiator	M/I	polymer	M_{nCal} (kDa)[b]	M_n (kDa)[c]	M_w/M_n[c]	DL (%)[d]
1	CPT-*S*-*S*-OH	100	CPT-*S*-*S*-poly(**2**)$_{100}$	20.7	22.3	1.06	1.6
2	CPT-*S*-*S*-OH	50	CPT-*S*-*S*-poly(**2**)$_{50}$	10.6	11.1	1.06	3.1
3	CPT-*S*-*S*-OH	20	CPT-*S*-*S*-poly(**2**)$_{20}$	4.6	4.8	1.05	7.3
4	CPT-*S*-*S*-OH	10	CPT-*S*-*S*-poly(**2**)$_{10}$	2.6	2.6	1.05	13.4
5	mPEG$_{5k}$	20	mPEG$_{5k}$-poly(**2**)$_{20}$	9.0	9.7	1.08	
6	mPEG$_{5k}$	10	mPEG$_{5k}$-poly(**2**)$_{10}$	7.0	7.3	1.08	
7	mPEG$_{2k}$	20	mPEG$_{2k}$-poly(**2**)$_{20}$	6.0	6.2	1.07	
8	mPEG$_{2k}$	10	mPEG$_{2k}$-poly(**2**)$_{10}$	4.0	4.2	1.07	
9	CPT	50	CPT-poly(**2**)$_{50}$	10.4	11.8	1.09	3.0
10	CPT	20	CPT-poly(**2**)$_{20}$	4.4	6.0	1.08	5.8
11	CPT	10	CPT-poly(**2**)$_{10}$	2.1	3.5	1.08	9.9

[a]Entries 1−8: Dimethylaminopyridine and dichloromethane were used as the catalyst and solvent, respectively. Entries 9−11: (BDI-EI)ZnN(TMS)$_2$ and tetrahydrofuran were used as the catalyst and solvent, respectively. [b]Calculated from M/I ratio with complete monomer conversion. [c]Determined by GPC. [d]DL = drug loading.

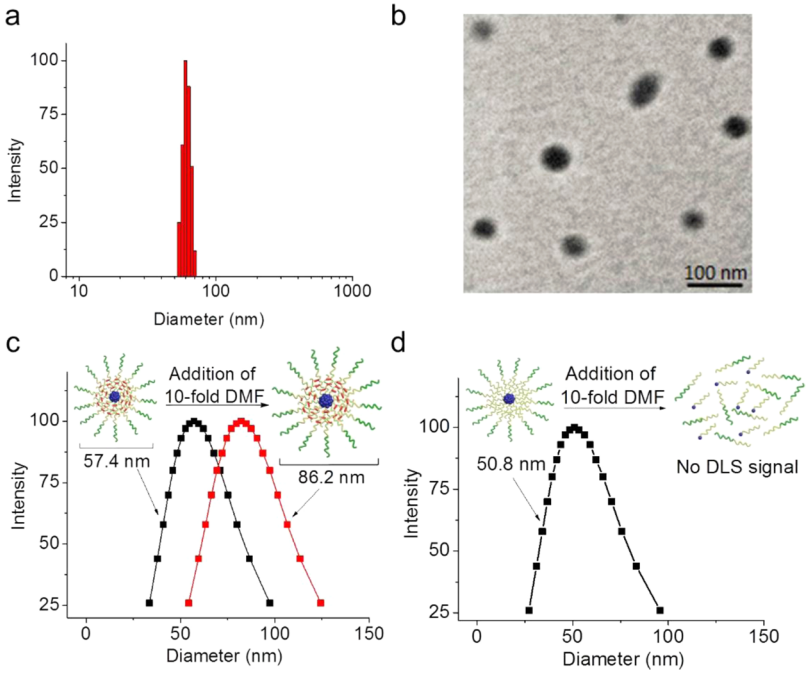

Figure 1. DLS (a) and TEM (b) characterizations of CCL micelles prepared from mPEG$_{2k}$-poly(**2**)$_{20}$ and CPT-*S*-*S*-poly(**2**)$_{20}$. (c) DLS showed swelling of CCL micelles upon dilution by 10-fold volume of DMF. (d) DLS showed dissolution of UCL micelles upon dilution by 10-fold volume of DMF.

lane-2,4-dione (tyrosine(alkynyl)-OCA, **2**)[54] to yield drug−polyester conjugate (CPT-*S*-*S*-poly(**2**)) with the redox-responstive linker between CPT and polyester. After coprecipitation with monomethoxy poly(ethylene glycol)-*b*-poly(**2**) (mPEG-poly(**2**)) to form micelles, bis(azidoethyl) disulfide linker was added to cross-link the core to stabilize the micelles. With surface PEGylation and core cross-linking, the micelles exhibited excellent stability under physiological conditions. Once internalized by cancer cells, high concentration of intracellular GSH disrupted the micellar structure and released the drug rapidly due to the existence of disulfide bonds in both the CPT−polyester conjugate and the cross-linker, leading to enhanced cytotoxicity against cancer cells compared with nondegradable CCL micelles.

RESULTS AND DISCUSSIONS

Preparation and Characterization of CCL Micelles. We first synthesized redox-cleavable CPT−polyester conjugate (CPT-*S*-*S*-poly(**2**)) and the control CPT−polyester conjugate (CPT-poly(**2**)) (Scheme 1a). To make CPT-*S*-*S*-poly(**2**), CPT was modified with 2-hydroxyethyl disulfide to yield **1**. The terminal hydroxyl group of **1** was used to initiate controlled ring-opening polymerization of **2** with 4-dimethylaminopyridine as the catalyst.[54,55] Drug−polyester conjugates with controlled molecular weights (MWs) and narrow molecular weight distributions (MWDs) were obtained (Table 1). Drug loading could be readily controlled for this class of drug−polymer conjugates by controlling the polymer chain length in living polymerization. Drug loading as high as 13.4% was achieved. We selected CPT-*S*-*S*-poly(**2**)$_{20}$ (prepared at the monomer/initiator ratio of 20, entry 3, Table 1) for micellization in our study. CPT-poly(**2**) conjugates were prepared via CPT/Zn-catalyst initiated polymerization as previously reported by us,[8,56,57] and CPT-poly(**2**)$_{20}$ (prepared at the monomer/initiator ratio of 20, entry 10, Table 1) was selected as the control. mPEG-poly(**2**)s were prepared similarly

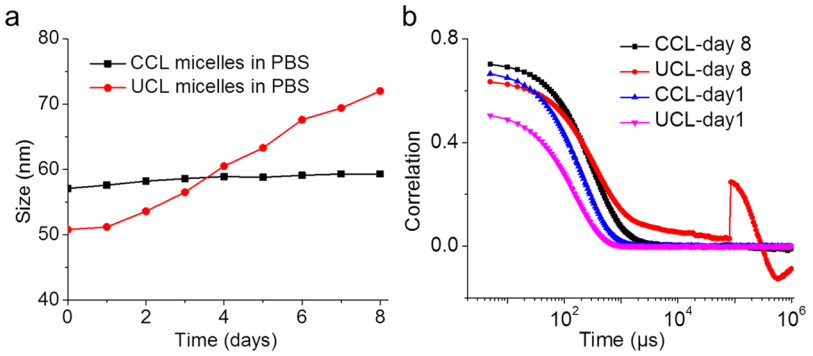

Figure 2. (a) Stability of CCL and UCL micelles in PBS (pH 7.4) at 37 °C. (b) Correlation function changes of CCL and UCL micelles after incubation in PBS for 8 days.

Scheme 2. Degradation and CPT Release of CCL1, CCL2, and CCL3 in the Presence of DTT

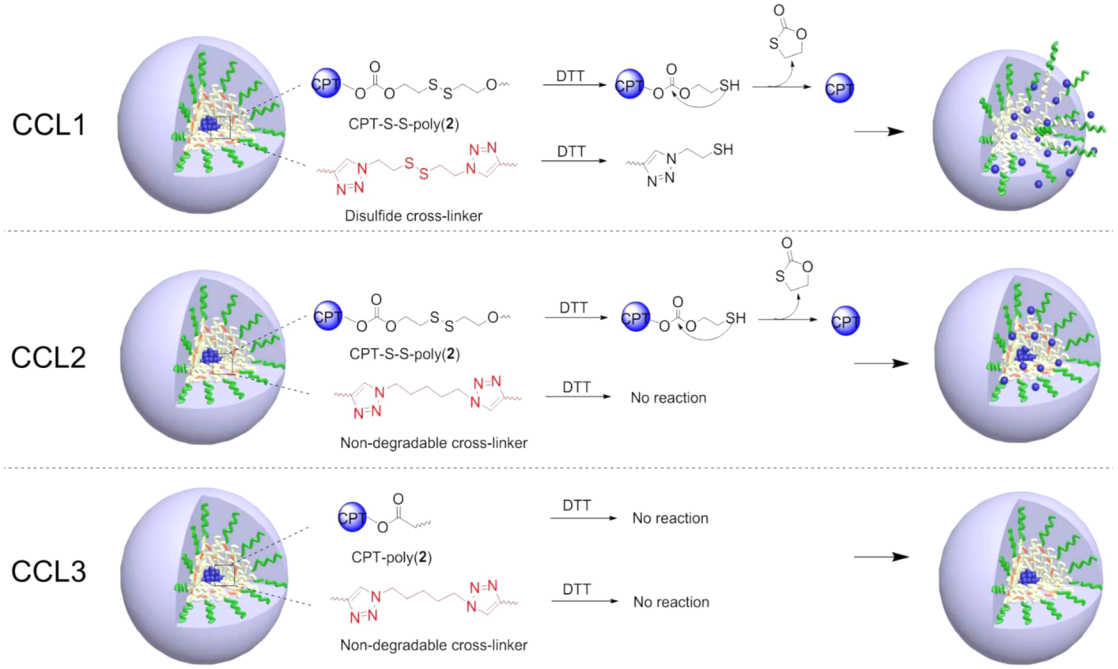

using mPEG (2k or 5k) as the initiator (Table 1),[54,55] and $mPEG_{2k}$-poly(**2**)$_{20}$ (entry 7, Table1) was selected for micellization. We then coprecipitated CPT-*S*-*S*-poly(**2**)$_{20}$ with mPEG-poly(**2**)$_{20}$ to form PEGylated micelles (Scheme 1b). CPT-*S*-*S*-poly(**2**)$_{20}$, mPEG-poly(**2**)$_{20}$, and diazide cross-linker were mixed in DMF at 1:1:1.4 molar ratio, and the mixture was added dropwise to vigorously stirred DI water, followed by the addition of copper chloride and sodium ascorbate to cross-link the core of the formed micelles via azide−alkyne click chemistry.[58] The resulting CCL micelles were analyzed by dynamic light scattering (DLS) (Figure 1a) and transmission electron microscopy (TEM) (Figure 1b). The micelles formed of CPT-*S*-*S*-poly(**2**)$_{20}$ and $mPEG_{2k}$-poly(**2**)$_{20}$ had a hydrodynamic size of 57.4 ± 0.6 nm in diameter by DLS measurement and a core size of 40.1 ± 3.8 nm by TEM.

To confirm the formation of CCL micelles, we prepared uncross-linked (UCL) micelles without adding the disulfide cross-linker during the preparation process as the control. Because both PEG-poly(**2**) and CPT-*S*-*S*-poly(**2**) are highly soluble in DMF with a solubility of 50 and 500 mg/mL, respectively, a simple solubility test of the micelles would readily differentiate CCL and UCL micelles and validate the CCL feature of the formed micelles. CCL and UCL micelles were lyophilized and then added to DMF at a final concentration of total polymer of 10 mg/mL. As a result, CCL micelles were insoluble in DMF, while UCL micelles could be readily dissolved in DMF. We also used a dilution assay to verify the structural difference between CCL and UCL micelles. The micelles were first prepared in aqueous solution and then diluted with a 10-fold volume of DMF. The size change of the micelles was monitored by DLS (Figure 1c,d). CCL micelle maintained its structure, but its size increased from 57.4 to 86.2 nm upon dilution due to the swelling of the hydrophobic core of the micelles by DMF.[56] In contrast, the structure of control UCL micelle was completely disrupted upon dilution with DMF due presumably to the dissolution of poly(**2**) core in DMF. To further demonstrate the cross-linked structure of CCL micelles, we monitored the change of light-scattering intensity of these two micelle solutions upon gradual addition of DMF (Figure S4 in the Supporting Information). As expected, CCL micelle solution experienced much slower decrease in light scattering intensity than UCL micelles, further substantiating its enhanced micellar stability by core-cross-linking. Moreover, ^{1}H NMR spectrum of lyophilized CCL micelles prepared from $mPEG_{2k}$-poly(**2**)$_{20}$/

dx.doi.org/10.1021/bm401086d | *Biomacromolecules* 2013, 14, 3706−3712

Table 2. Structure and Size of CCL1, CCL2, CCL3, and UCL Micelles

	components					
	CPT-*S*-*S*-poly(**2**)$_{20}$	CPT-poly(**2**)$_{20}$	disulfide cross-linker[a]	nondegradable cross-linker[b]	size (nm)[c]	PDI[c]
CCL1	×		×		57.4 ± 2.0	0.138 ± 0.009
CCL2	×			×	55.3 ± 2.8	0.165 ± 0.013
CCL3		×		×	59.2 ± 2.6	0.194 ± 0.011
UCL	×				50.8 ± 2.3	0.208 ± 0.008

[a]Bis(azidoethyl) disulfide. [b]1,5-Diazidopentane. [c]Determined by DLS. Measurement was done in triplicate. Results represent average ± standard deviation. mPEG$_{2k}$-poly(**2**)$_{20}$ was used for the preparation of these micelles.

CPT-*S*-*S*-poly(**2**)$_{20}$ in DMSO-d_6 showed much lower proton peaks of polyester backbone than that of the PEG segment, which could be ascribed to enclosing of hydrophobic polyesters within the hydrophilic PEG segments (Figure S3 in the Supporting Information).

Stability of CCL Micelles. Next, we compared the stability of CCL and UCL micelles under physiological conditions. CCL and UCL micelles were dispersed in phosphate buffer solution (PBS, pH 7.4) and incubated at 37 °C. CCL micelles showed negligible change from 57.4 to 59.3 nm after they were incubated in PBS for 8 days, while the size of UCL micelles increased significantly from 50.8 to 72.0 nm over the same period (Figure 2a), demonstrating the higher stability of CCL micelles over UCL micelles. We also tracked the change of correlation functions of CCL and UCL micelles by DLS measurement. After being incubated in PBS for 8 days, the rate of decay for the correlation function of UCL micelles became much slower, indicating the formation of large aggregates. The correlation function of CCL micelles, however, showed nearly no change over the same period (Figure 2b). Instability of UCL micelles can be explained by vulnerable micellar structure under physiological ionic strength.[57] Once the UCL micellar structure was disrupted, the exposed hydrophobic cores would easily aggregate. In comparison, core of CCL micelles was stably cross-linked and shielded within the hydrophilic PEG segments and had little chance for intermicellar hydrophobic interaction to form aggregates. These results demonstrated that CCL micelles have greatly enhanced stability under physiological conditions.

Redox-Responsive Degradation of CCL Micelles. To verify the redox-degradable property of CCL micelles, we investigated dithiothreitol (DTT)-induced structural change of three types of CCL micelles: CCL1, CCL2, and CCL3 (Scheme 2 and Table 2). CCL1 has disulfide bonds both in the CPT−polyester conjugate and in the cross-linker. CCL2 has disulfide bond in the CPT−polyester conjugate but does not have disulfide bond in the cross-linker. CCL3 has disulfide bond neither in CPT−polyester conjugate nor in the cross-linker. The molecular weight of the polymers used for making micelles and the alkyne−azide ratio was controlled to be the same for all three CCL micelles. CCL1 showed size reduction from 57.4 to 49.8 nm after treatment with 10 mM DTT for 6 h. After further dilution with 10-fold volume of DMF, DTT-treated CCL1 showed no DLS signal, indicating that the disulfide bonds in the micelle cores had been degraded and the micelles were disassembled (Figure 3a). In contrast, CCL2 and CCL3 only showed some swelling after the same DTT treatment and 10-fold DMF dilution because of the non-degradability of the cross-linked structure (Figure S5 in the Supporting Information). CCL1 was lyophilized and redispersed in DMF to further prove the redox-responsive degradation of CCL1 in the presence of DTT, showing visually

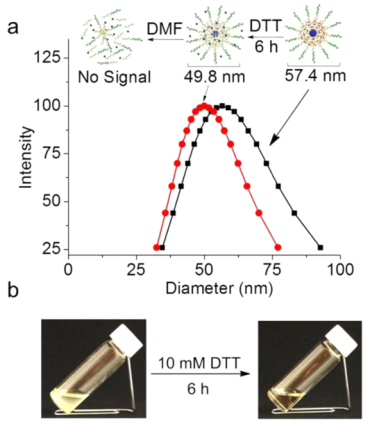

Figure 3. (a) Redox-degradability of CCL1 in the presence of 10 mM DTT. (b) Photographs of lyophilized CCL1 in DMF before and after treatment with 10 mM DTT (37 °C).

turbid solution. After incubation with 10 mM DTT at 37 °C for 6 h, the solution became completely clear due to the cleavage of the cross-linked network and the formation of DMF-soluble uncross-linked micelles or polymers (Figure 3b).

Reduction-Triggered Drug Release. We next investigated the drug release profiles of CCL micelles in response to the redox trigger. First, we compared CPT release rate of CCL1 in the presence of different concentrations of DTT (Figure 4a). After 24 h of incubation, 15.9 ± 1.5, 65.6 ± 2.5, and 81.7 ± 2.9% of CPT were released in the presence of 1, 5, and 10 mM DTT, respectively, while almost no CPT release was observed in the absence of DTT, which demonstrated the redox-responsive drug release property of CCL1. In comparison, CCL2 showed much slower CPT release profile compared with CCL1 and released only 20% of CPT in the presence of 10 mM DTT for 24 h (Figure 4b). Although CPT-*S*-*S*-poly(**2**) in CCL2 can be cleaved by DTT, the nondegradable, hydrophobic, cross-linked core prevented DTT from reaching the CPT-*S*-*S*-poly(**2**) disulfide bonds in the micellar core and reduced the outward diffusion of the cleaved drug from the core, thus greatly slowing the overall release kinetics of CPT. CCL3 showed essentially no CPT release in the presence of 10 mM DTT after 4 days of incubation because of the nondegradability of the CPT-poly(**2**) conjugate upon DTT treatment (Scheme 1a).

Redox-Responsive Cytotoxicity. To demonstrate the proliferation inhibition capability of CCL micelles, we investigated the cytotoxicity of micelles against MCF-7 human breast cancer cells using MTT (3-(4,5-dimethylthiazol-2-yl)-2, 5-diphenyltetrazolium bromide) colorimetric assay. MCF-7 cells were treated with free CPT or CCL micelles at various concentrations of CPT equivalent for 48 h, and the cell viability was shown in Figure 5a. CCL1 with redox-

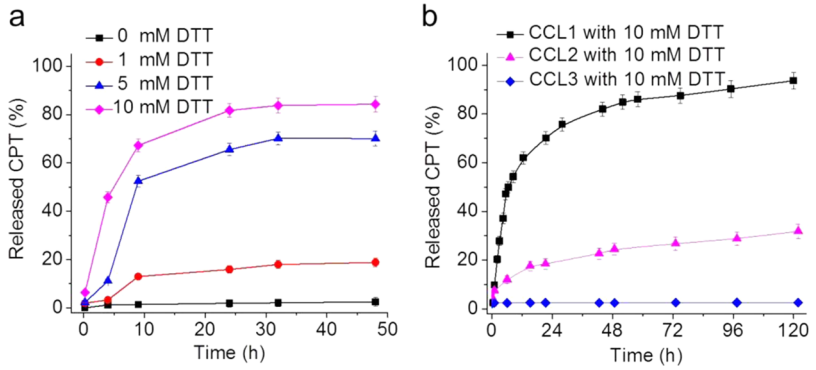

Figure 4. (a) In vitro CPT release profiles of CCL1 in PBS (pH 7.4, 37 °C) in the presence of 0, 1, 5, and 10 mM DTT, respectively. (b) In vitro CPT release profiles of CCL1, CCL2, and CCL3 in PBS (pH 7.4, 37 °C) in the presence of 10 mM DTT. Data are presented as average ± standard deviation, $n = 3$.

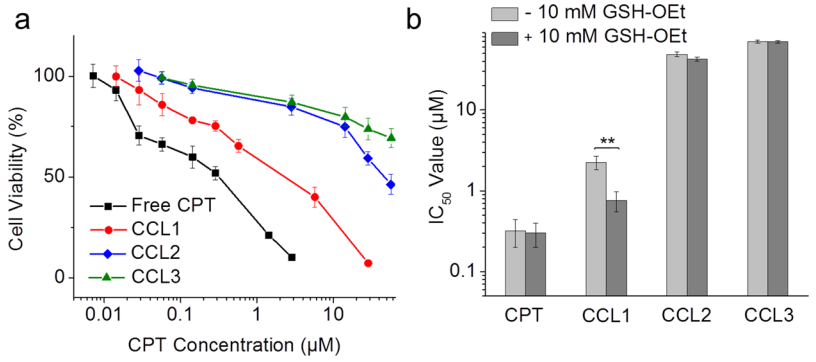

Figure 5. (a) Viability of MCF-7 breast cancer cells after treatment with free CPT or CCL micelles at various concentrations of CPT equivalent for 48 h. (b) IC_{50} values of free CPT, CCL1, CCL2, and CCL3 with or without GSH-OEt pretreatment. Statistical significance was assessed by two-sample unpaired Student's t test; $0.01 < p \leq 0.05$ and $p \leq 0.01$ are considered to be statistically significant and highly significant and are denoted as "*" and "**", respectively.

responsive linkers for both micelle structure and drug conjugates showed highest cytotoxicity among all three CCL micelles tested, with an IC_{50} value of 2.24 μM. CCL2 showed much lower cytotoxicity against MCF-7 cells, with an IC_{50} value of 48.7 μM. CCL3, which has the lowest cytotoxicity, only reduced the cell viability to 69.1 ± 4.6% at the micellar CPT concentration of 50.0 μM. The highest cytotoxicity of CCL1 could be ascribed to the disassembly of the cross-linked micelle and rapid release of CPT in cancer cells with high intracellular concentration of GSH.

To further investigate the redox-responsive cytotoxicity of CCL micelles, we evaluate the viability of micelle-treated cells with the addition of GSH level regulators. It has been reported that glutathione monoester (GSH-OEt) can increase the intracellular concentration of GSH via hydrolyzation after entering the cells.[53,59] Prior to the addition of CCL micelles, cells were pretreated with 10 mM GSH-OEt for 4 h. The IC_{50} value of CCL1 against MCF-7 cancer cells decreased significantly from 2.24 to 0.76 μM with the pretreatment of GSH-OEt (Figure 5b). In comparison, GSH-OEt caused negligible difference in the IC_{50} value of CCL2 and CCL3, which could be explained by less or no responsiveness to reductive environment of CCL2 and CCL3 compared with CCL1.

CONCLUSIONS

In conclusion, a new class of redox-responsive CCL micelles has been developed for anticancer drug delivery. CCL micelles showed enhanced stability over UCL micelles under physiological conditions and exhibited rapid degradation and concurrent drug release in reductive environment. In vitro cytotoxicity study demonstrated the enhanced anticancer activity of the redox-responsive CCL micelles than non-responsive micelles. Increased solubility and stability of the hydrophobic drug, reductive-triggered rapid drug release, combined with degradable polyester backbone make this micelle system a promising candidate for drug delivery application.

ASSOCIATED CONTENT

Supporting Information

Experimental details including NMR spectra, DLS, TEM, light scattering intensity, correlation function, and MTT results. This material is available free of charge via the Internet at http://pubs.acs.org.

AUTHOR INFORMATION

Corresponding Author

*E-mail: jianjunc@illinois.edu.

Notes

The authors declare no competing financial interest.

ACKNOWLEDGMENTS

This work is supported by NIH Director's New Innovator Award 1DP2OD007246 and NSF DMR 1309525.

REFERENCES

(1) Nasongkla, N.; Shuai, X.; Ai, H.; Weinberg, B. D.; Pink, J.; Boothman, D. A.; Gao, J. *Angew. Chem., Int. Ed.* **2004**, *43*, 6323−6327.
(2) Zhang, Z.; Xiong, X.; Wan, J.; Xiao, L.; Gan, L.; Feng, Y.; Xu, H.; Yang, X. *Biomaterials* **2012**, *33*, 7233−7240.
(3) Bhargava, P.; Tu, Y.; Zheng, J. X.; Xiong, H.; Quirk, R. P.; Cheng, S. Z. D. *J. Am. Chem. Soc.* **2007**, *129*, 1113−1121.
(4) Tong, R.; Cheng, J. *Polym. Rev.* **2007**, *47*, 345−381.
(5) Tong, R.; Tang, L.; Cheng, J. J. *Dev. Appl. Anticancer Nanomed.* **2012**, 31−46.
(6) Tong, R.; Christian, D. A.; Tang, L.; Cabral, H.; Baker, J. R.; Kataoka, K.; Discher, D. E.; Cheng, J. J. *MRS Bull.* **2009**, *34*, 422−431.
(7) Koo, H.; Lee, S.; Na, J. H.; Kim, S. H.; Hahn, S. K.; Choi, K.; Kwon, I. C.; Jeong, S. Y.; Kim, K. *Angew. Chem., Int. Ed.* **2012**, *51*, 11836−11840.
(8) Tong, R.; Cheng, J. *Angew. Chem., Int. Ed.* **2008**, *47*, 4830−4834.
(9) Shuai, X.; Merdan, T.; Schaper, A. K.; Xi, F.; Kissel, T. *Bioconjugate Chem.* **2004**, *15*, 441−448.
(10) Fan, J. Q.; Zeng, F.; Wu, S. Z.; Wang, X. D. *Biomacromolecules* **2012**, *13*, 4126−4137.
(11) Wang, K.; Liu, Y.; Yi, W.-J.; Li, C.; Li, Y.-Y.; Zhuo, R.-X.; Zhang, X.-Z. *Soft Matter* **2013**, *9*, 692−699.
(12) Salahuddin, S.; Renaudet, O.; Reymond, J.-L. *Org. Biomol. Chem.* **2004**, *2*, 1471−1475.
(13) Kim, Y.; Liemmawal, E. D.; Pourgholami, M. H.; Morris, D. L.; Stenzel, M. H. *Macromolecules* **2012**, *45*, 5451−5462.
(14) Koo, A. N.; Min, K. H.; Lee, H. J.; Lee, S.-U.; Kim, K.; Chan Kwon, I.; Cho, S. H.; Jeong, S. Y.; Lee, S. C. *Biomaterials* **2012**, *33*, 1489−1499.
(15) Wang, K.; Luo, G.-F.; Liu, Y.; Li, C.; Cheng, S.-X.; Zhuo, R.-X.; Zhang, X.-Z. *Polym. Chem.* **2012**, *3*, 1084−1090.
(16) Liu, Y.; Wang, Y.; Wang, Y.; Lu, J.; Piñón, V.; Weck, M. *J. Am. Chem. Soc.* **2011**, *133*, 14260−14263.
(17) Wu, Y.; Chen, W.; Meng, F.; Wang, Z.; Cheng, R.; Deng, C.; Liu, H.; Zhong, Z. *J. Controlled Release* **2012**, *164*, 338−345.
(18) Wei, R.; Cheng, L.; Zheng, M.; Cheng, R.; Meng, F.; Deng, C.; Zhong, Z. *Biomacromolecules* **2012**, *13*, 2429−2438.
(19) Li, Y.; Yang, D.; Adronov, A.; Gao, Y.; Luo, X.; Li, H. *Macromolecules* **2012**, *45*, 4698−4706.
(20) Crielaard, B. J.; Rijcken, C. J. F.; Quan, L.; van der Wal, S.; Altintas, I.; van der Pot, M.; Kruijtzer, J. A. W.; Liskamp, R. M. J.; Schiffelers, R. M.; van Nostrum, C. F.; Hennink, W. E.; Wang, D.; Lammers, T.; Storm, G. *Angew. Chem., Int. Ed.* **2012**, *51*, 7254−7258.
(21) Liu, S.; Weaver, J. V. M; Tang, Y.; Billingham, N. C.; Armes, S. P.; Tribe, K. *Macromolecules* **2002**, *35*, 6121−6131.
(22) Read, E. S.; Armes, S. P. *Chem. Commun.* **2007**, 3021−3035.
(23) Yue, J.; Wang, R.; Liu, S.; Wu, S.; Xie, Z.; Huang, Y.; Jing, X. *Soft Matter* **2012**, *8*, 7426−7435.
(24) Danquah, M.; Fujiwara, T.; Mahato, R. I. *J. Polym. Sci., Part A: Polym. Chem.* **2013**, *51*, 347−362.
(25) Yang, Z.; Zheng, S.; Harrison, W. J.; Harder, J.; Wen, X.; Gelovani, J. G.; Qiao, A.; Li, C. *Biomacromolecules* **2007**, *8*, 3422−3428.
(26) van Nostrum, C. F. *Soft Matter* **2011**, *7*, 3246−3259.
(27) Talelli, M.; Iman, M.; Varkouhi, A. K.; Rijcken, C. J. F.; Schiffelers, R. M.; Etrych, T.; Ulbrich, K.; van Nostrum, C. F.; Lammers, T.; Storm, G.; Hennink, W. E. *Biomaterials* **2010**, *31*, 7797−7804.
(28) Kuang, H.; Wu, S.; Meng, F.; Xie, Z.; Jing, X.; Huang, Y. *J. Mater. Chem.* **2012**, *22*, 24832−24840.
(29) Fleige, E.; Quadir, M. A.; Haag, R. *Adv. Drug Delivery Rev.* **2012**, *64*, 866−884.
(30) Wang, Y.; Byrne, J. D.; Napier, M. E.; DeSimone, J. M. *Adv. Drug Delivery Rev.* **2012**, *64*, 1021−1030.
(31) Ge, Z.; Liu, S. *Chem. Soc. Rev.* **2013**, *42*, 7289−7325.
(32) Chiang, W.-H.; Ho, V. T.; Huang, W.-C.; Huang, Y.-F.; Chern, C.-S.; Chiu, H.-C. *Langmuir* **2012**, *28*, 15056−15064.
(33) Pan, Y.-J.; Chen, Y.-Y.; Wang, D.-R.; Wei, C.; Guo, J.; Lu, D.-R.; Chu, C.-C.; Wang, C.-C. *Biomaterials* **2012**, *33*, 6570−6579.
(34) Ke, C.-J.; Chiang, W.-L.; Liao, Z.-X.; Chen, H.-L.; Lai, P.-S.; Sun, J.-S.; Sung, H.-W. *Biomaterials* **2013**, *34*, 1−10.
(35) Binauld, S.; Scarano, W.; Stenzel, M. H. *Macromolecules* **2012**, *45*, 6989−6999.
(36) Oberoi, H. S.; Laquer, F. C.; Marky, L. A.; Kabanov, A. V.; Bronich, T. K. *J. Controlled Release* **2011**, *153*, 64−72.
(37) Hsiao, M.-H.; Lin, K.-H.; Liu, D.-M. *Soft Matter* **2013**, *9*, 2458−2466.
(38) Hu, X.; Li, H.; Luo, S.; Liu, T.; Jiang, Y.; Liu, S. *Polym. Chem.* **2013**, *4*, 695−706.
(39) Sugihara, S.; Ito, S.; Irie, S.; Ikeda, I. *Macromolecules* **2010**, *43*, 1753−1760.
(40) Pan, P.; Fujita, M.; Ooi, W.-Y.; Sudesh, K.; Takarada, T.; Goto, A.; Maeda, M. *Langmuir* **2012**, *28*, 14347−14356.
(41) Wan, X.; Liu, T.; Liu, S. *Langmuir* **2011**, *27*, 4082−4090.
(42) Matsumoto, S.; Christie, R. J.; Nishiyama, N.; Miyata, K.; Ishii, A.; Oba, M.; Koyama, H.; Yamasaki, Y.; Kataoka, K. *Biomacromolecules* **2008**, *10*, 119−127.
(43) Zhao, L.; Yan, Y.; Huang, J. *Langmuir* **2012**, *28*, 5548−5554.
(44) Tao, Y.; Han, J.; Ye, C.; Thomas, T.; Dou, H. *J. Mater. Chem.* **2012**, *22*, 18864−18871.
(45) Wang, C.; Chen, Q.; Wang, Z.; Zhang, X. *Angew. Chem., Int. Ed.* **2010**, *49*, 8612−8615.
(46) Chien, M.-P.; Thompson, M. P.; Lin, E. C.; Gianneschi, N. C. *Chem. Sci.* **2012**, *3*, 2690−2694.
(47) Deng, L.; Wang, G.; Ren, J.; Zhang, B.; Yan, J.; Li, W.; Khashab, N. M. *RSC Adv.* **2012**, *2*, 12909−12914.
(48) Chau, Y.; Tan, F. E.; Langer, R. *Bioconjugate Chem.* **2004**, *15*, 931−941.
(49) Chau, Y.; Padera, R. F.; Dang, N. M.; Langer, R. *Int. J. Cancer* **2006**, *118*, 1519−1526.
(50) Cajot, S.; Lautram, N.; Passirani, C.; Jérôme, C. *J. Controlled Release* **2011**, *152*, 30−36.
(51) Yan, L. S.; Wu, W. B.; Zhao, W.; Qi, R. G.; Cui, D. M.; Xie, Z. G.; Huang, Y. B.; Tong, T.; Jing, X. B. *Polym. Chem.* **2012**, *3*, 2403−2412.
(52) Duong, H. T. T.; Huynh, V. T.; de Souza, P.; Stenzel, M. H. *Biomacromolecules* **2010**, *11*, 2290−2299.
(53) Koo, A. N.; Lee, H. J.; Kim, S. E.; Chang, J. H.; Park, C.; Kim, C.; Park, J. H.; Lee, S. C. *Chem. Commun.* **2008**, *0*, 6570−6572.
(54) Zhang, Z. H.; Yin, L. C.; Xu, Y. X.; Tong, R.; Lu, Y. B.; Ren, J.; Cheng, J. J. *Biomacromolecules* **2012**, *13*, 3456−3462.
(55) Zhang, Z.; Yin, L.; Zhang, Y.; Xu, Y.; Tong, R.; Zhou, Q.; Ren, J.; Cheng, J. *ACS Macro Lett.* **2012**, *2*, 40−44.
(56) Tong, R.; Cheng, J. *J. Am. Chem. Soc.* **2009**, *131*, 4744−4754.
(57) Tong, R.; Cheng, J. *Bioconjugate Chem.* **2009**, *21*, 111−121.
(58) Kolb, H. C.; Finn, M. G.; Sharpless, K. B. *Angew. Chem., Int. Ed.* **2001**, *40*, 2004−2021.
(59) Hong, R.; Han, G.; Fernández, J. M.; Kim, B.-j.; Forbes, N. S.; Rotello, V. M. *J. Am. Chem. Soc.* **2006**, *128*, 1078−1079.